Electronic Supplementary Material (ESI) for ChemComm.
This journal is © The Royal Society of Chemistry 2023

Electronic Supplementary Information

$Cs[B_3O_3F_2(OH)_2]$: Discovery of a hydroxyfluorooxoborate guided by selective organic-inorganic transformation

Ziqi Chen,[a,b] Fuming Li,[a,b] Jian Han[a,b] Zhihua Yang,[a,b] Shilie Pan*,[a,b] Miriding Mutailipu,*,[a,b]

[a] Research Center for Crystal Materials, CAS Key Laboratory of Functional Materials and Devices for Special Environments, Xinjiang Technical Institute of Physics and Chemistry, CAS, Urumqi, People's Republic of China

[b] Center of Materials Science and Optoelectronics Engineering, University of Chinese Academy of Sciences, Beijing, People's Republic of China

*Corresponding authors, E-mails: slpan@ms.xjb.ac.cn and miriding@ms.xjb.ac.cn

Experimental Section

Single crystals and polycrystalline. $Cs[B_3O_3F_2(OH)_2]$ crystals can be obtained by high-temperature solution method in a closed system. Polycrystalline sample of $Cs[B_3O_3F_2(OH)_2]$ was obtained by solid-state reaction. A mixture of $CsBF_4$ (0.176 g, 0.801 mmol), CsF (0.122 g, 0.801 mmol), B_2O_3 (0.028 g, 0.400 mmol), and H_3BO_3 (0.074 g, 1.201 mmol) were loaded into a tidy silica glass tube (Φ10 mm × 100 mm) and the tube was flame-sealed under 10^{-3} Pa. The tube was heated to 350 °C in 3 h, and held at this temperature for 24 h; and then cooled to 30 °C with a rate of 1.0 °C /h. The polycrystalline samples of $Cs[B_3O_3F_2(OH)_2]$ were synthesized via conventional solid-state reactions at an open system according to its stoichiometric of CsF and H_3BO_3. The mixtures were ground thoroughly, placed in separate platinum crucibles, and gradually heated to 100 °C and held at this temperature in air for 24 h. The powder XRD of $Cs[B_3O_3F_2(OH)_2]$ was performed at different temperatures, it can be seen that $Cs[B_3O_3F_2(OH)_2]$ is stable up to ~300 °C. The final decomposition product is $Cs_2B_4O_7$ at the temperature higher than ~500 °C.

Characterization. Powder XRD data were collected with a Bruker D2 PHASER diffractometer (Cu Kα radiation with λ = 1.5418 Å, 2θ = 10 to 70 °, scan step width = 0.02 °, and counting time= 1 s/step). The single-crystal XRD data were collected on a Bruker D8 Venture diffractometer using Mo Kα radiation (λ = 0.71073 Å) at room temperature. The intensity, reduction and cell refinement were carried out on Bruker SAINT.[1] All the structures were solved by direct method and refined through the full-matrix least-squares fitting on F^2 with OLEX2 software.[2] These structures were verified by virtue of ADDSYM algorithm from PLATON.[3] Infrared spectroscopy was carried out on a Shimadzu IR Affinity-1 Fourier transform infrared spectrometer in the 400-4000 cm^{-1} range. UV−vis−NIR diffuse-reflectance spectroscopy data in the wavelength range of 190-2500 nm were recorded at room temperature using a powder sample of $Cs[B_3O_3F_2(OH)_2]$ on a Shimadzu SolidSpec-3700 DUV spectrophotometer. Solid-state ^1H MAS NMR spectra were recorded with a single pulse excitation, a 90° pulse length of 3.4 μs and a recycle delay of 4 s were applied to obtain quantitative results. The ^{19}F and ^{11}B MAS NMR experiments were performed on a Bruker Avance III 500 WB

(11.75 T) spectrometer operating at a frequency of 470.96 and 160.61 MHz for ^{19}F and ^{11}B, respectively. A commercial DVT quadruple resonance H/F/X/Y 2.5 mm CP/MAS probe was used with a spinning frequency of 30.0 kHz. Solid-state ^{19}F MAS NMR spectra were recorded with a single pulse excitation using a 90-degree pulse width of 1.9 us (pi/2) and a recycle delay of 5 s to obtain quantitative results. There is no fluorine background from the H/F/X/Y probehead. ^{19}F chemical shifts were determined using a solid external reference, Poly(tetrafluoroethylene) (PTFE). The CF_2 groups of PTFE resonate at -122 ppm relative to tetramethylsilane (TMS). ^{11}B MAS NMR spectra was recorded, with a single pulse excitation using a short pulse length (0.32 us) to obtain quantitative results, and a recycle delay of 10 s (the tip angle was pi/12). ^{11}B chemical shifts were referenced using H_3BO_3 1 M in solution as an external reference (19.6 ppm). The presence of B-F bonds was checked employing $^{11}B\{^{19}F\}$-REDOR NMR spectroscopy, which enables the determination of the heteronuclear ^{11}B-^{19}F dipole coupling and hence the evaluation of internuclear distances.

Calculation details

The electronic structure and optical property were calculated by using the DFT method implemented in the CASTEP package.[4] During the calculation, the generalized gradient approximation (GGA) with Perdew-Burke-Ernzerhof (PBE) functional was adopted.[5a] Under the norm-conserving pseudopotential (NCP), the following orbital electrons were treated as valence electrons: H:$1s^1$, B:$2s^22p^1$, O:$2s^22p^4$, F:$2s^22p^4$, and Cs:$5s^25p^66s^1$. The kinetic energy cutoffs of 940 eV were chosen, and the numerical integration of the Brillouin zone was performed using a 2 × 3 × 3 Monkhorst-Pack *k*-point sampling. The other calculation parameters and convergent criteria were the default values of the CASTEP code. In order to clarify the contribution of different units to the birefringence of $Cs[B_3O_3F_2(OH)_2]$, bonding electron density differences ($\Delta\rho$) of $[BO_2F_2]$, $[CsO_6F_5]$ and $[BO_2(OH)]$ were calculated using the REDA method.[5b]

Table S1. Crystallographic data and structural refinement parameters of $Cs[B_3O_3F_2(OH)_2]$.

Compound	$Cs[B_3O_3F_2(OH)_2]$
Formula weight	285.36
Crystal system	Monoclinic
Space group	$P2_1/c$
a (Å)	7.4498(5)
b (Å)	5.9711(4)
c (Å)	15.5448(12)
β (°)	β = 100.466(3)
V (Å^3)	679.98(8)
Z	4
d_{cal} (g/cm^3)	2.787
μ (mm^{-1})	5.451
F(000)	520
Crystal size (mm^3)	0.13 × 0.12 × 0.1
Theta range for data collection	2.66 to 27.51°
Limiting indices	$-9 \leq h \leq 9$, $-7 \leq k \leq 7$, $-20 \leq l \leq 20$
Reflections collected / unique	11704/1568 [R(int) = 0.0758]
Completeness to theta = 27.51°	99.9 %
Data / restraints / parameters	1568 / 0 / 108
Goodness-of-fit on F^2	1.067
R_1 (I>2sigma(I)])[a]	0.0299
wR_2 (I >2sigma(I)])[a]	0.0463
R_1 (all data)[a]	0.0475
wR_2 (all data)[a]	0.0501
Largest diff. peak and hole e.Å^{-3}	0.570 and -0.588

[a]$R_1 = \Sigma||F_o| - |F_c||/\Sigma|F_o|$ and $wR_2 = [\Sigma w(F_o^2 - F_c^2)^2 / \Sigma w F_o^4]^{1/2}$ for $F_o^2 > 2\sigma(F_o^2)$

Table S2. Atomic coordinates, equivalent isotropic displacement parameters and bond valence sum (BVS) for $Cs[B_3O_3F_2(OH)_2]$. U_{eq} is defined as one-third of the trace of the orthogonalized U_{ij} tensor.

Atoms	*x/a*	*y/b*	*z/c*	U_{eq}(Å^2)	BVS
Cs(1)	0.0913(1)	0.2791(1)	0.1149(1)	0.037(1)	1.048
B(1)	0.2194(6)	0.2714(8)	0.3674(3)	0.032(1)	3.026
B(2)	0.4225(6)	0.5727(8)	0.3396(3)	0.033(1)	3.077
B(3)	0.5452(6)	0.2749(8)	0.4332(3)	0.032(1)	3.091
O(1)	0.2539(3)	0.4820(4)	0.3279(2)	0.035(1)	2.009
O(2)	0.5726(3)	0.4655(4)	0.3882(2)	0.037(1)	2.103
O(3)	0.3762(3)	0.1878(4)	0.4284(2)	0.034(1)	1.856
O(4)	0.6933(4)	0.1821(6)	0.4847(2)	0.044(1)	1.199
O(5)	0.4613(4)	0.7719(5)	0.3063(2)	0.046(1)	1.144
F(1)	0.1713(3)	0.1065(4)	0.3004(2)	0.044(1)	0.824
F(2)	0.0708(3)	0.2894(4)	0.4103(2)	0.044(1)	0.911
H(1)	0.3770(60)	0.8370(70)	0.2870(30)	0.034(14)	-
H(2)	0.6770(70)	0.0760(90)	0.5110(40)	0.070(20)	-

Table S3. Selected bond distances (Å) and <O-B-F> bond angles (°) for $Cs[B_3O_3F_2(OH)_2]$.

Bond	Length	Bond	Length
Cs(1)-F(1)	3.018(3)	B(1)-F(2)	1.397(5)
Cs(1)-O(2)#1	3.134(3)	B(1)-F(1)	1.430(5)
Cs(1)-F(2)#2	3.161(2)	B(1)-O(1)	1.442(5)
Cs(1)-F(2)#3	3.182(3)	B(1)-O(3)	1.453(5)
Cs(1)-F(1)#4	3.212(3)	B(2)-O(5)	1.349(5)
Cs(1)-F(2)#4	3.275(2)	B(2)-O(1)	1.350(5)
Cs(1)-O(4)#5	3.280(3)	B(2)-O(2)	1.387(5)
Cs(1)-O(5)#1	3.336(3)	B(3)-O(3)	1.352(5)
Cs(1)-O(1)#2	3.374(3)	B(3)-O(4)	1.358(5)
Cs(1)-O(4)#6	3.415(4)	B(3)-O(2)	1.370(5)
Cs(1)-O(1)	3.528(3)	O(5)-H(1)	0.75(4)
		O(4)-H(2)	0.78(5)

Type	Angle	Type	Angle
F(2)-B(1)-F(1)	106.6(3)	O(5)-B(2)-O(1)	124.1(4)
F(2)-B(1)-O(1)	110.8(3)	O(5)-B(2)-O(2)	114.1(4)
F(1)-B(1)-O(1)	109.4(4)	O(1)-B(2)-O(2)	121.8(4)
F(2)-B(1)-O(3)	109.1(3)	O(3)-B(3)-O(4)	121.6(4)
F(1)-B(1)-O(3)	107.7(3)	O(3)-B(3)-O(2)	121.0(4)
O(1)-B(1)-O(3)	113.1(3)	O(4)-B(3)-O(2)	117.4(4)

Symmetry transformations used to generate equivalent atoms:

#1 -x+1,y-1/2,-z+1/2 #2 -x,y-1/2,-z+1/2 #3 x,-y+1/2,z-1/2
#4 -x,y+1/2,-z+1/2 #5 x-1,-y+1/2,z-1/2 #6 -x+1,y+1/2,-z+1/2

Table S4. Anisotropic displacement parameters (Å^2) for $Cs[B_3O_3F_2(OH)_2]$.

Atom	U_{11}	U_{22}	U_{33}	U_{23}	U_{13}	U_{12}
Cs(1)	32(1)	41(1)	38(1)	4(1)	4(1)	6(1)
B(1)	27(2)	35(3)	33(3)	7(2)	2(2)	-3(2)
B(2)	35(3)	32(3)	34(3)	5(2)	10(2)	-1(2)
B(3)	29(2)	31(2)	35(3)	-1(2)	3(2)	-2(2)
O(1)	28(2)	36(2)	40(2)	10(1)	4(1)	-1(1)
O(2)	27(2)	34(2)	48(2)	10(1)	3(1)	-5(1)
O(3)	29(1)	36(2)	36(2)	10(1)	2(1)	-4(1)
O(4)	28(2)	44(2)	56(2)	17(2)	-5(2)	-4(1)
O(5)	37(2)	37(2)	66(2)	20(2)	10(2)	1(2)
F(1)	47(2)	44(1)	38(2)	0(1)	-2(1)	-6(1)
F(2)	33(1)	52(2)	51(2)	12(1)	18(1)	2(1)

Table S5. Bonding electron density difference (Δρ) and contribution percent *w* (%) of different units in $Cs[B_3O_3F_2(OH)_2]$ calculated by the REDA method.

Units	Δρ (×10^4)	*w* (%)
$[B(1)O_2(OH)]$	106.9	67.76%
$[B(2)O_2(OH)]$	49.6	31.44%
$[BO_2F_2]$	3.5	2.22%
$[CsO_6F_5]$	-2.4	-1.52%

Table S6. Examples of Cs-[Ph_4P/[Ph_3MeP] substitution.

No.	Cs	Space group	[Ph_4P]/[Ph_3MeP]	Space group	Ref.
1	Cs_2NpCl_6	$R\bar{3}m$	$(Ph_4P)_2NpCl_6$	$P\bar{1}$	6
2	$CsTi_2F_9$	C2/c	$(Ph_4P)_2Ti_4F_{18}$	$P\bar{1}$	7
3	$Cs[NTf_2]$	C2/c	$[Ph_4P][NTf_2]$	$C2/c$	8
4	$Cs_2NpO_2Cl_4$	C2/m	$[Ph_4P]_2NpO_2Cl_4$	$P\bar{1}$	9
5	$Cs_2PuO_2Cl_4$	C2/m	$[Ph_4P]_2PuO_2Cl_4$	$P\bar{1}$	10
6	$CsUF_6$	$R\bar{3}$	$[Ph_4P]UF_6$	$I\bar{4}$	11
7	$Cs_3Mg(BH_4)_5$	$I4/mcm$	$[Ph_4P]_2[Mg(BH_4)_4]$	-	12
8	$Cs[Cu(CF_3)_2]$	C2/m	$[Ph_4P]^+[Cu(CF_3)_2]^-$	$Pbcn$	13
9	$Cs[Al(BH_4)_4]$	$I4_1/amd$	$[Ph_3MeP][Al(BH_4)_4]$	$Pca2_1$	14
10	$Cs_3[Sb_2I_9]$	$P6_3/mmc$	$[Ph_3MeP]_3[Sb_2I_9]$	$P2_1/c$	15
11	$CsCu_2I_3$	$Cmcm$	$[Ph_3MeP]_2[Cu_4I_6]$	$R\bar{3}c$	16

Table S7. Real-space atom-cutting analysis of calculated birefringence in $Cs[B_3O_3F_2(OH)_2]$

Cut unit	Birefringence(@1064nm)
None	0.049
Cs	0.049
$[B_3O_3F_2(OH)_2]$	0.001

Figure S1. X-ray powder diffraction patterns of experimental and calculated results for $Cs[B_3O_3F_2(OH)_2]$.

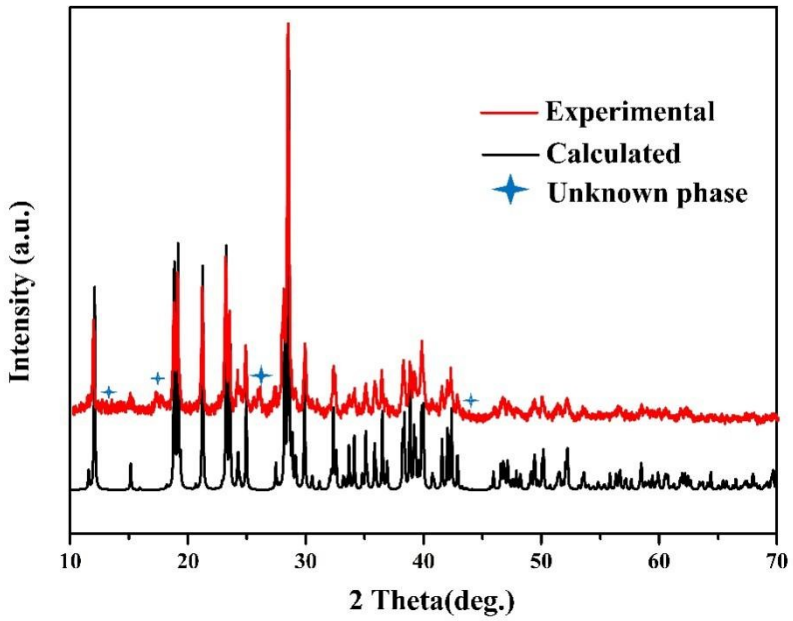

Figure S2. The experimental and calculated XRD patterns of $Cs[B_3O_3F_2(OH)_2]$ at different temperature.

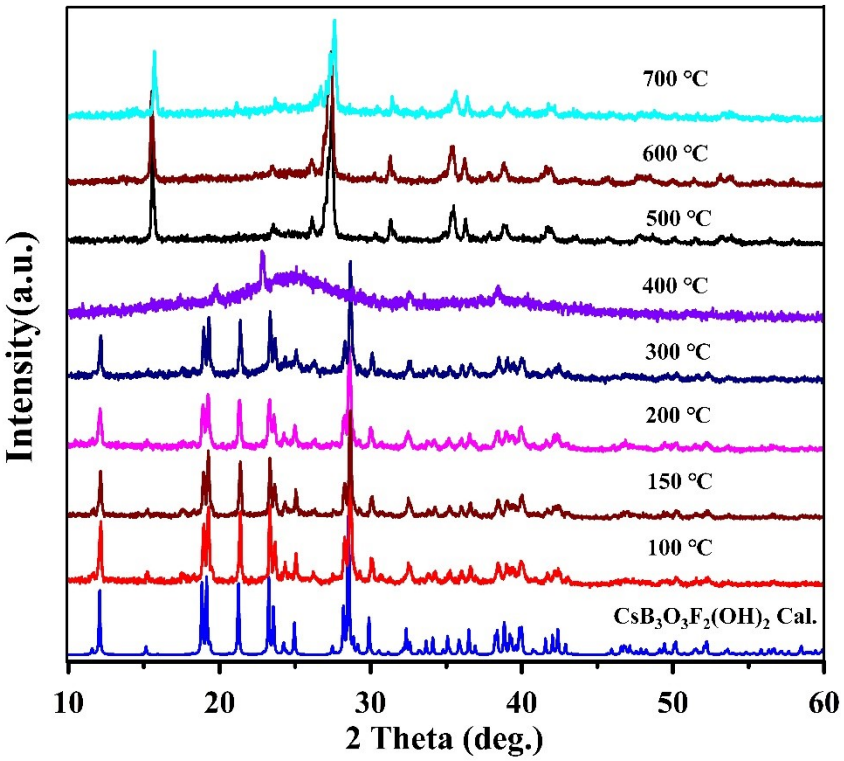

Figure S3. (**a**) The basic structural units of $[BO_2F_2]$ and $[BO_2OH]$. (**b**) The 1D pseudo $[B_6O_6F_4(OH)_4]_\infty$ *zigzag* chain. (**c, d**) The $[CsO_6F_5]$ polyhedra and 1D $[CsO_4F_3]_\infty$ chains polymerized by the cationic polyhedra.

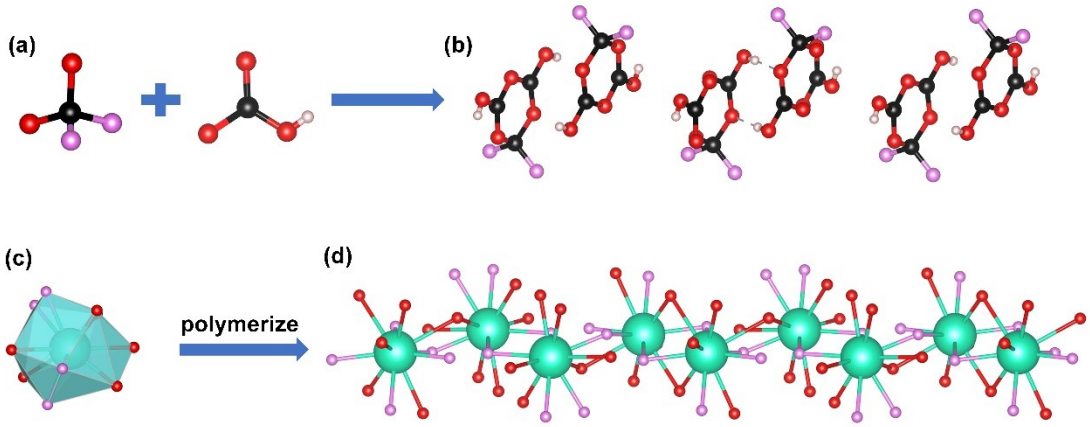

Figure S4. The final structure of $Cs[B_3O_3F_2(OH)_2]$ constructed by $[CsO_4F_3]_\infty$ and pseudo $[B_6O_6F_4(OH)_4]_\infty$ chains.

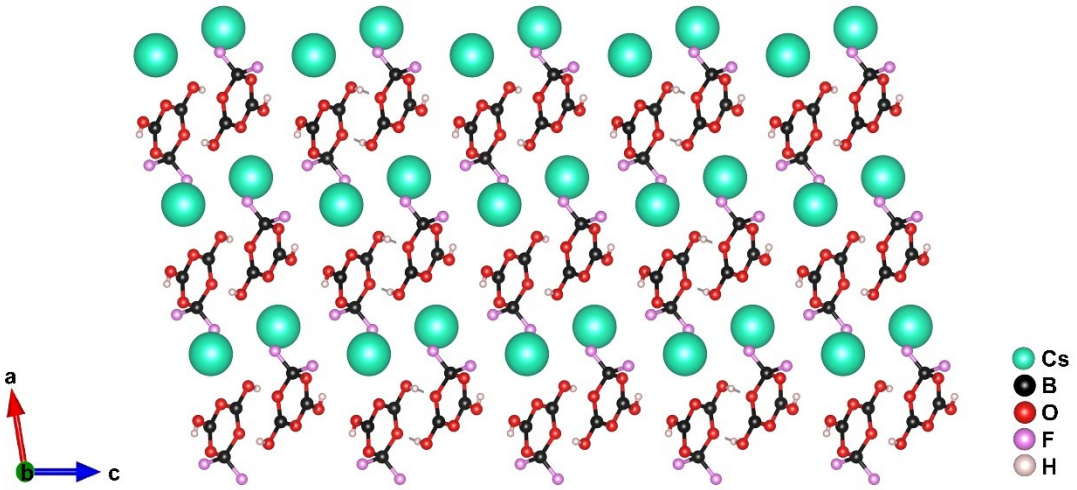

Figure S5. IR spectrum of $Cs[B_3O_3F_2(OH)_2]$.

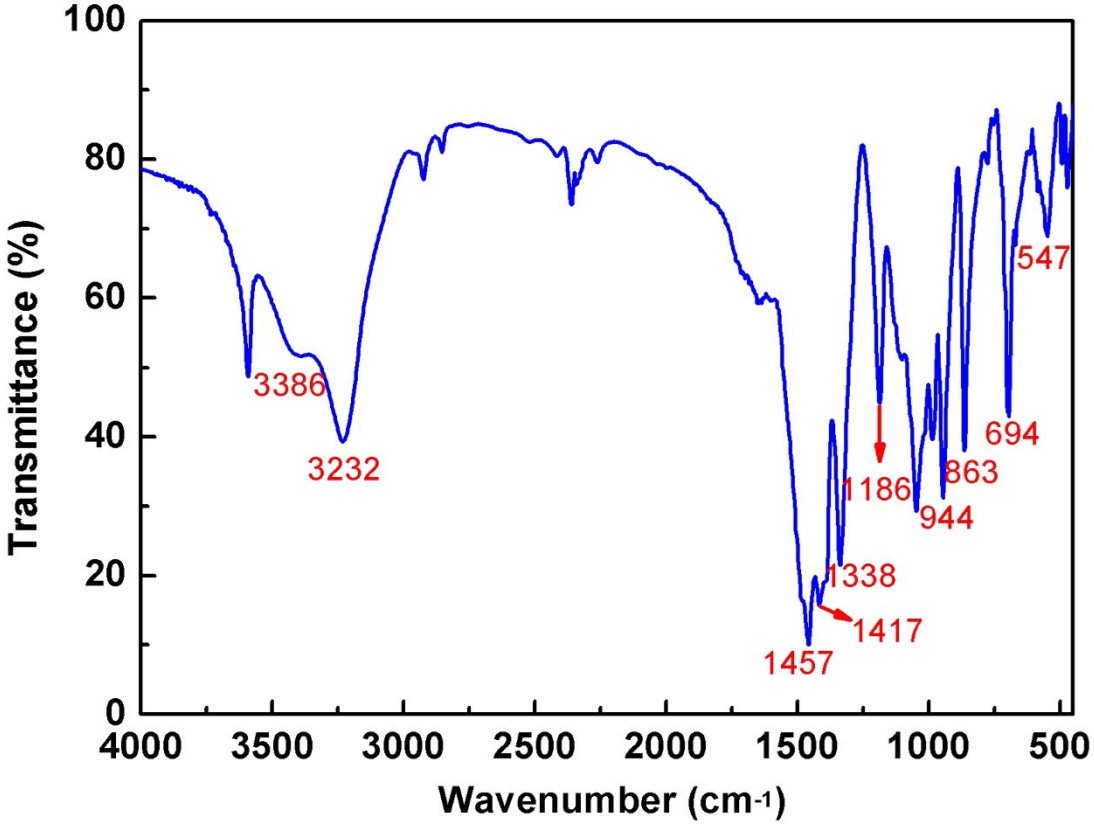

Figure S6. UV-VIS-NIR spectrum of $Cs[B_3O_3F_2(OH)_2]$.

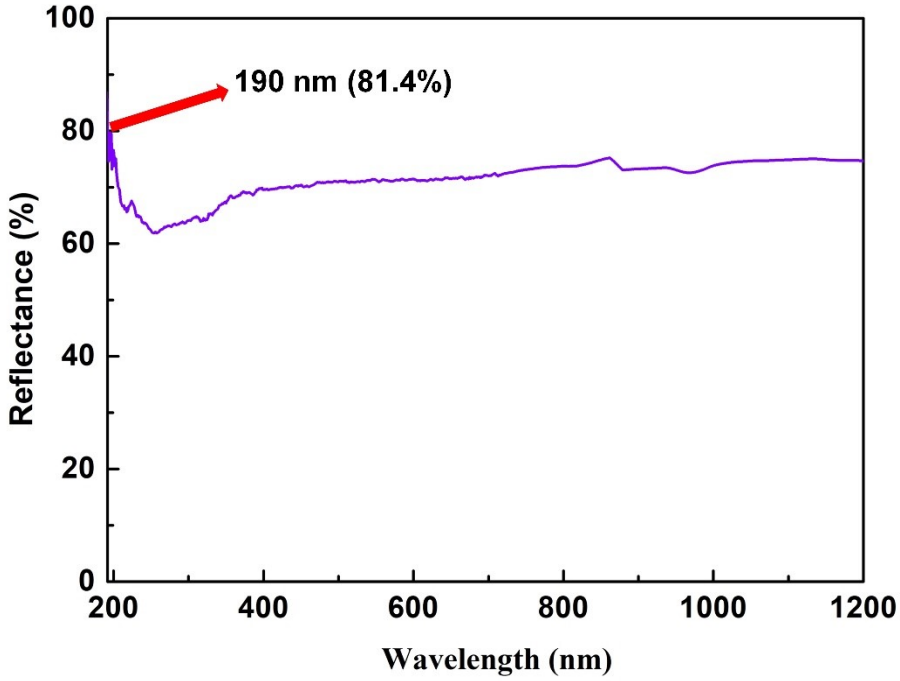

Figure S7. The electronic structure of $Cs[B_3O_3F_2(OH)_2]$ based on GGA method.

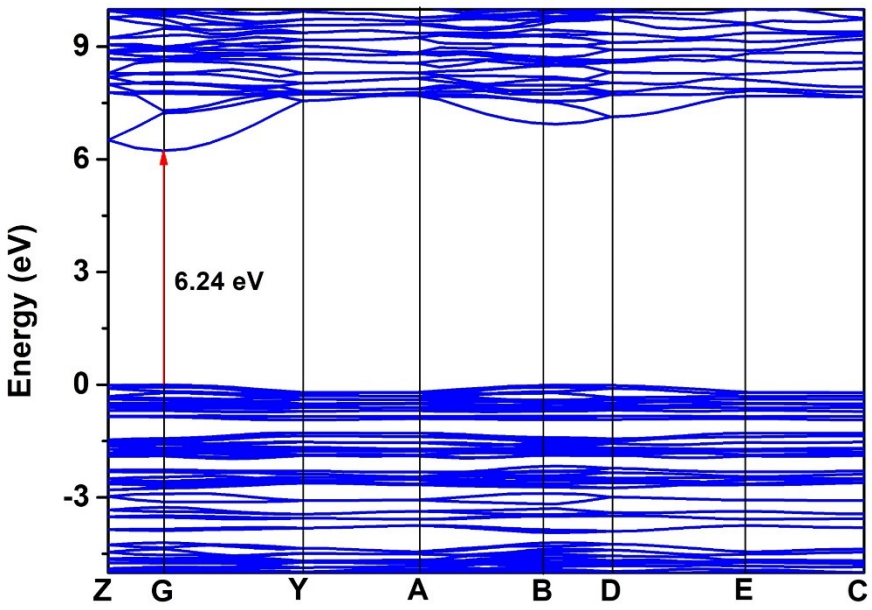

Figure S8. The total and partial density of states of $Cs[B_3O_3F_2(OH)_2]$.

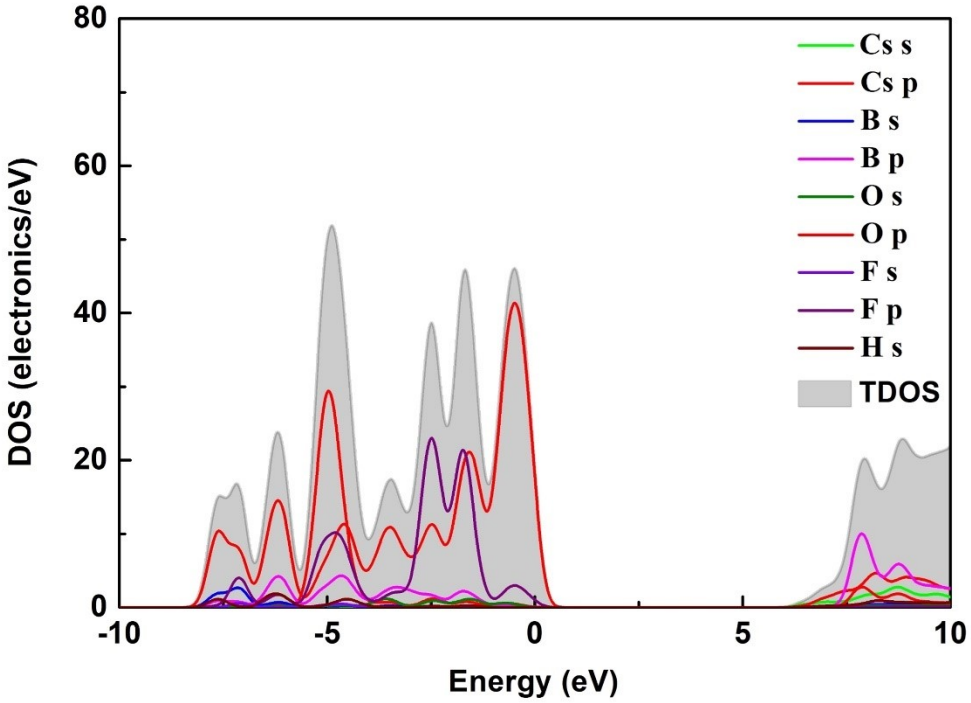

Figure S9. The calculated birefringence curve of $Cs[B_3O_3F_2(OH)_2]$

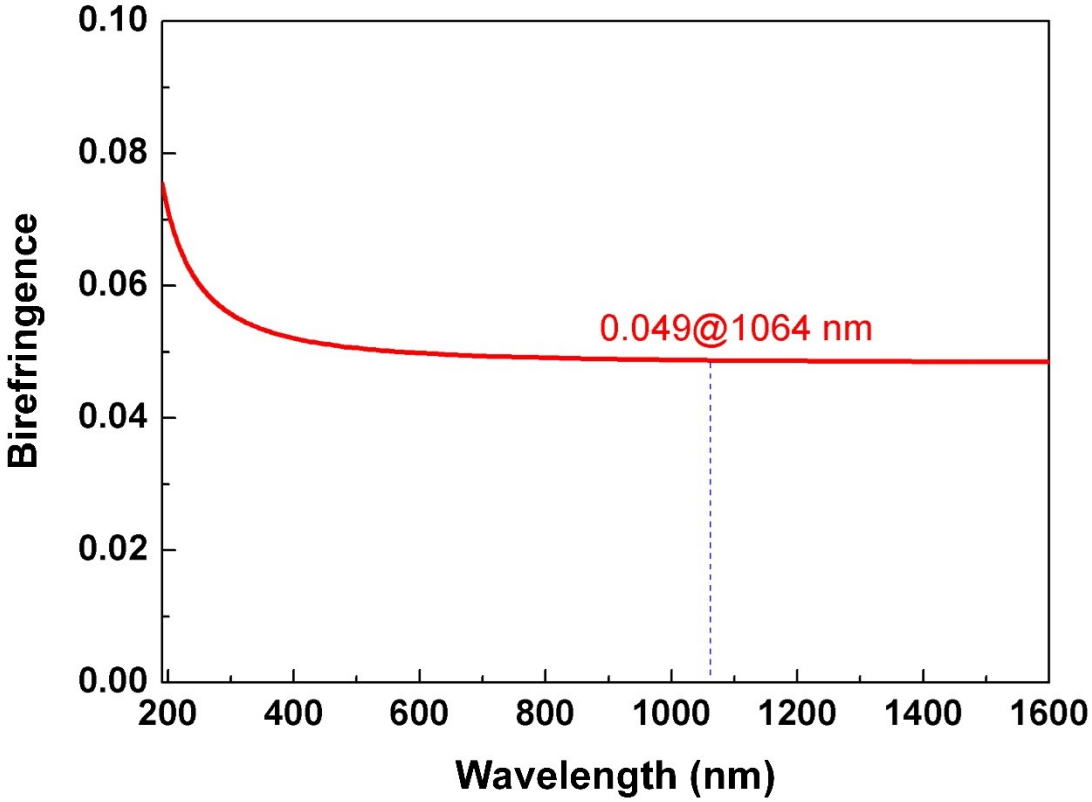

References

1. SAINT, Version 7.60A,Bruker Analytical X-ray Instruments, Inc.,Madison, WI, 2008.
2. O. V. Dolomanov, L. J. Bourhis, R. J. Gildea, J. A. Howard and H. Puschmann, *J. Appl. Crystallogr.*, 2009, **42**, 339-341.
3. A. Spek, *J. Appl. Crystallogr.*, 2003, **36**, 7-13.
4. S. J. Clark, M. D. Segall, C. J. Pickard, P. J. Hasnip, M. I. Probert, K. Refson and M. C. Payne, *Z Kristallogr Cryst Mater*, 2005, **220**, 567-570.
5. (a) J. P. Perdew, K. Burke and M. Ernzerhof, *Phys. Rev. Lett.*, 1996, **77**, 3865; (b) B. H. Lei, Z. H. Yang and S. L. Pan, *Chem. Commun.*, 2017, **53**, 2818-2821.
6. S. G. Minasian, K. S. Boland, R. K. Feller, A. J. Gaunt, S. A. Kozimor, I. May, S. D. Reilly, B. L. Scott and D. K. Shuh, *Inorg. Chem.*, 2012, **51**, 5728-5736.
7. Z. Mazej and E. Goreshnik, *Inorg. Chem.*, 2009, **48**, 6918-6923.
8. (a) C. G. Cassity, A. Mirjafari, N. Mobarrez, K. J. Strickland, R. A. O'Brien and J. H. Davis, *Chem. Commun.*, 2013, **49**, 7590-7592; (b) M. Scheuermeyer, M. Kusche, F. Agel, P. Schreiber, F. Maier, H.-P. Steinrück, J. H. Davis, F. Heym, A. Jess and P. Wasserscheid, *New J. Chem.*, 2016, **40**, 7157-7161.
9. M. P. Wilkerson, C. A. Arrington, J. M. Berg and B. L. Scott, *J. Alloys Compd.*, 2007, **444**, 634-639.
10. D. D. Schnaars and R. E. Wilson, *Inorg. Chem.*, 2013, **52**, 14138-14147.
11. W. Grape and E. Stumpp, *Inorg. Nucl. Chem. Lett.*, 1979, **15**, 137-142.
12. W. Wegner, T. Jaroń, M. Dobrowolski, M. Cyrański and W. Grochala, *Dalton Trans.*, 2016, **45**, 14370-14377.
13. H. Liu and Q. L. Shen, *Org. Chem. Front.*, 2019, **6**, 2324-2328.
14. I. Dovgaliuk, D. A. Safin, N. A. Tumanov, F. Morelle, A. Moulai, R. Černý, Z. Łodziana, M. Devillers and Y. Filinchuk, *ChemSusChem*, 2017, **10**, 4725-4734.
15. V. Sharutin, V. Senchurin, O. Sharutina and B. Kunkurdonova, *Russ. J. Gen. Chem.*, 2011, **81**, 2235-2241.
16. G. A. Bowmaker, G. R. Clark and D. P. Yuen, *Dalton Trans.*, 1976, **26**, 2329-2334.